Wind Washing Effects on Mineral Wool Insulated Sheathings

Randy Van Straaten, MASc, PEng
Student Member ASHRAE

John Straube, PhD, PEng
Associate Member ASHRAE

Trevor Trainor, MASc

Antoine Habellion, MEng, MAS

ABSTRACT

Wind washing *is wind-driven air movement through or behind thermal insulation within enclosures. This bulk movement of air increases heat loss, resulting in increased energy consumption, risk of condensation on cooled surfaces, and increased space-heating loads. Previous studies have investigated airflow bypassing the insulation through gaps, around insulation boards, and through low-density fibrous insulation products. The impact of wind washing on well-installed mineral wool board products used outside the air barrier as continuous insulation has not been previously studied in detail. This paper presents a methodology for predicting wind washing impacts and laboratory measurement of heat loss impacts for insulation products exposed to cavity airflows.*

It is recommended that average winter wind speeds (or ASHRAE mean coincident wind speed) be used for wind washing analysis. A method is presented for adjusting wind speeds for sheltering and height impacts based on approaches used in structural wind load calculations. Hourly average air speeds as high as 0.1 and 0.7 m/s (0.4 and 2.4 ft/s) were predicted using simple airflow network analysis for well-ventilated brick cladding and slot panels, respectively. Analysis of full-scale wind tunnel pressure tap data for a small house was used to predict vinyl siding cavity air speeds as high as 0.5 m/s (1.5 ft/s). Heat flow measurements were taken for a number of insulation products in a purpose-built apparatus. Of the mineral wool board samples tested, only the 25 and 50 mm (1 and 2 in.) thick 70 kg/m^3 (4.4 pcf) samples showed measurable wind washing impact. This impact was as much as 0.03 RSI (R-0.2) reduction of thermal performance. Hence, wind washing impacts are expected to be small for well-installed mineral wool board continuous insulation.

INTRODUCTION

Wind washing is wind-driven air movement through or behind thermal insulation within enclosures. This bulk movement of air increases heat loss, resulting in increased energy consumption, risk of condensation on cooled surfaces, and increased space-heating loads. Previous research has shown that wind washing of air-permeable insulations is most significant for installations with

- higher air velocities along the insulation surface due to higher wind exposure and/or more open cladding systems (Bankvall 1978; Henning 1983; Taylor and Phillips 1983; Uvsløkk 1996);
- higher insulation air permeability, typically correlating with lower density and/or less thickness (Bankvall 1978; Henning 1983; Taylor and Phillips 1983; Yarbrough and Tooe 1983; Tanner and Ghazi 1996);
- installation imperfections resulting in air gaps around and behind the insulation (Bankvall 1978; Hens et al. 2001); and
- greater scouring of insulation due to eddies in the cavity airflow, and/or greater air momentum from direct wind exposure (Bankvall 1978; Berlad 1979; Silberstein 1991; Deseyve and Bednar 2005; Janssen and Hens 2007).

Figure 1 illustrates the process of wind washing, and Figure 2 illustrates two measures to limit it: air cavity compart-

Randy Van Straaten is a senior research engineer at RDH Building Science Laboratories, Waterloo, Ontario, and a doctoral candidate in the Department of Civil and Environmental Engineering at Western University, London, Ontario. **John Straube** is a principal at RDH Building Science Laboratories and a professor in the Department of Civil Engineering, University of Waterloo, Waterloo, Ontario. **Trevor Trainor** is a building science researcher at RDH Building Science Laboratories. **Antoine Habellion** is a building science specialist at ROXUL Inc., Milton, Ontario.

mentalization and the application of a so-called "wind barrier" on the exterior of the insulation. Uvsløkk (1996) recommended a wind barrier air permeance no greater than 1.4E-5 $m^3/m^2 \cdot s \cdot Pa$, based on laboratory tests and field monitoring of a small test house. Mineral wool insulation boards used as sheathing have air permeances greater than Uvsløkk's recommendation, hence some designers choose to place wind barriers over top of them. However, Uvsløkk's recommendation was for a membrane installed over low-density fibreglass batt insulation without an air barrier. Therefore, his finding may not apply to unprotected insulation installed outboard of solid surfaces (often air barrier membranes), as is becoming common in North America. More air-permeable exterior insulation products may act as effective wind barriers themselves in such modern wall systems.

This paper presents a methodology for predicting wind washing impacts. The wind exposures are illustrated using a number of cold North American cities. The paper also presents laboratory measurement of heat loss impacts for insulation products exposed to cavity airflows. Based on these and the methodology, the impact of wind washing on mineral wool board products is predicted.

WIND SPEEDS FOR WIND WASHING ANALYSIS

Prevailing wind speed (WS) and direction vary depending on geographical location. Wind speeds for structural wind load requirements are published in building codes, but design speeds do not occur often and are too high for use in predicting wind washing impacts. Average annual wind speeds may also have limited suitability because higher wind speeds may occur in summer when wind washing is less of a concern. For heating degree day (HDD) energy analysis, one would ideally use a single HDD-weighted wind speed. However, such values are not readily available and the value would have a dependence on the balance temperature for the spaces being analyzed, complicating its derivation.

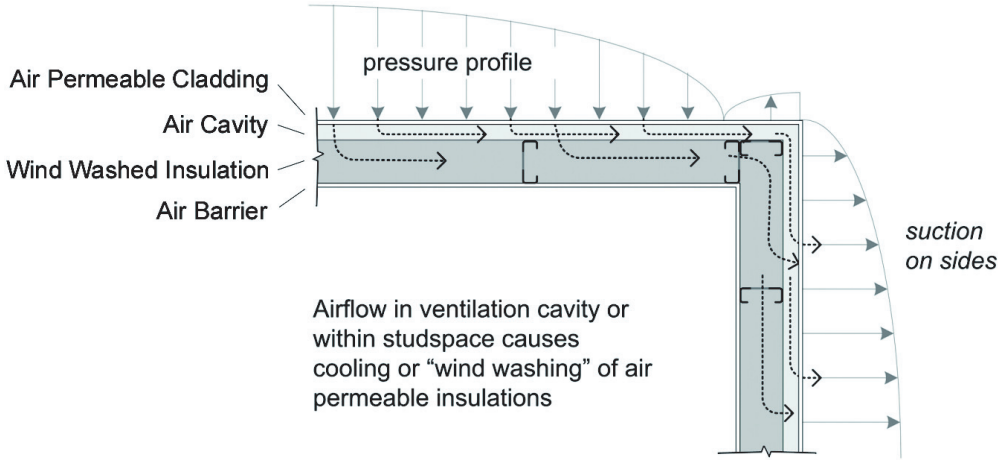

Figure 1 *Illustration of wind washing effects on a wall—plan view (adapted from Straube 2001).*

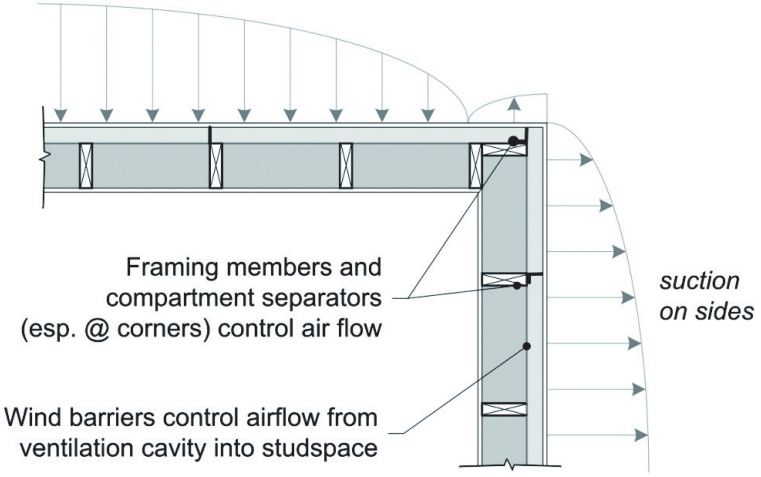

Figure 2 *Measures to address wind washing—plan view (adapted from Straube 2001).*

Three different approaches using ASHRAE climatic data (ASHRAE 2013) were considered for determining appropriate wind speeds for wind washing analysis. The first approach considered was to use mean January wind speeds and dry-bulb temperatures. This method is the simplest approach but does not account for the coincidence of both cold temperatures and high wind speeds. The second approach is to use the highest wind speed (0.04%) for the coldest month of the year and the mean coincident dry-bulb (MCDB) temperatures associated with that wind speed. This approach accounts for both cold temperatures and high wind speeds but applies more weight to wind speed than to temperature. A third approach is to choose the heating design temperature (99.6%) and the mean coincident wind speed (MCWS) associated with that temperature. This approach is similar but applies more weight to temperature than to wind speed.

Table 1 lists these values for some cold North American cities. The coldest month with 0.04% wind speeds (3.5 h/yr) are 6 to 9 m/s (13 to 20 mph) greater than January averages. However, the 99.6% dry-bulb temperature is as much as 20°C (36°F) colder than the January average and as much as 30°C (54°F) colder than both the coldest month average temperature and the temperature coincident with 0.04% wind speeds. It is assumed that the significant temperature difference would result in the 99.6% dry-bulb condition being a worst-case peak heating load and condensation condition for most locations. Furthermore, the use of the MCWS has the advantage of correlating with the temperature typically used for heating load calculations. MCWS values are used in the analysis presented in this paper.

The wind speeds given in Table 1 are based on the data from anemometers placed at 10 m (32.8 ft) heights in open fields. Straube (1998) used wind speed adjustments from structural building code calculations to adjust the wind speeds in driving rain analysis to adjust for local sheltering by surrounding buildings and landscapes (hills, cliffs, etc.) as well as height. It is proposed to use a similar approach for wind washing analysis. The results of this approach are given in Table 2 for a small house in the suburbs, a small house in the countryside, and a tall building in a city centre, where height, h, and sheltering (captured by logarithmic exponent, α) affect wind exposure. These values are used to estimate height-dependent mean wind speed as follows:

$$U = WS(h/10\ \text{m})^{\alpha} \quad (1)$$

Table 1. Cold Weather Wind Speeds in ASHRAE Climatic Design Data Tables

Location	Average January		Coldest Month Wind Speed		Coldest Month Wind Speed		Mean Coincident Wind Speed	
	DB, °C (°F)	WS, m/s (mph)	MCDB, °C (°F)	0.04%WS, m/s (mph)	MCDB, °C (°F)	0.1% WS, m/s (mph)	99.6% DB, °C (°F)	MCWS, m/s (mph)
Toronto	–4.7 (24)	4.9 (11)	–4.7 (24)	14.2 (32)	–4.1 (25)	12.7 (28)	–18.1 (–1)	4.8 (11)
Chicago	–3.9 (25)	4.9 (11)	–0.5 (31)	12.1 (27)	–0.6 (31)	11.1 (25)	–18.6 (–3)	4.9 (11)
New York City	0.8 (33)	5.6 (13)	–1.3 (30)	14.2 (32)	–0.9 (30)	12.8 (29)	–10.1 (14)	7.4 (17)
Edmonton	–12 (10)	3.3 (8)	–2.9 (27)	11.6 (26)	–6.7 (20)	10.1 (23)	–32.6 (–27)	2.1 (5)
Denver	–0.3 (31)	3.8 (9)	4.0 (39)	13.4 (30)	2.3 (36)	11.9 (27)	–17.5 (1)	3.5 (8)

Table 2. Adjusted Wind Speeds for Sample Building Types

Location	MCWS Open Field h = 10 m (32.8 ft) m/s (mph)	Small House in Suburbs h = 2 m (6. 6ft) α = 0.25 m/s (mph)	Small House in Countryside h = 2 m (6.6 ft) α = 0.13 m/s (mph)	Large Building in City Centre h = 30 m (98 ft) α = 0.25 m/s (mph)
Toronto	4.8 (11)	3.2 (9)	3.8 (7)	9.1 (20)
Chicago	4.9 (11)	3.3 (9)	3.9 (7)	9.3 (21)
New York City	7.4 (17)	4.9 (13)	5.9 (11)	14.1 (32)
Edmonton	2.1 (5)	1.4 (4)	1.7 (3)	4.0 (9)
Denver	3.5 (8)	2.3 (6)	2.8 (5)	6.7 (15)

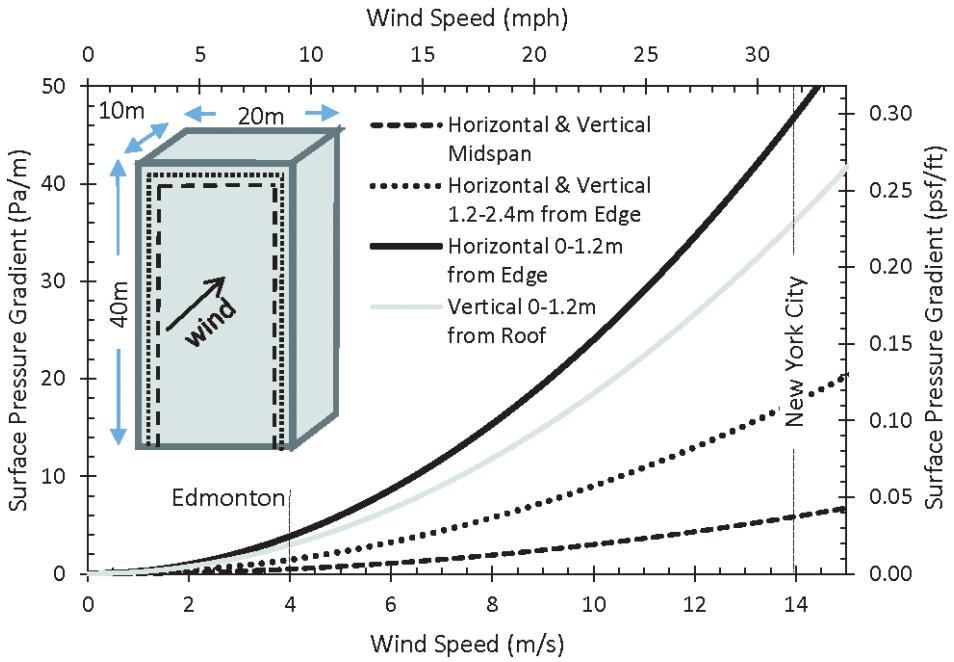

Figure 3 *Vertical and horizontal surface pressure gradients for a tall building.*

Table 3. Calculated Tall-Building Surface Pressure Gradients, Pa/m (psf/ft)

Location	Midspan	Tall Building in City Centre		
		1.2–2.4 m (4–8 ft) from Edge	Within 1.2 m (4 ft) of Edge	Within 1.2 m (4 ft) of Edge
	Horizontal/Vertical	Horizontal/Vertical	Horizontal	Vertical
Toronto	2.5 (0.016)	7.5 (0.048)	20.1 (0.128)	15.1 (0.096)
Chicago	2.6 (0.017)	7.9 (0.050)	20.9 (0.133)	15.7 (0.100)
New York City	6.0 (0.038)	17.9 (0.114)	47.7 (0.304)	35.8 (0.228)
Edmonton	0.5 (0.003)	1.4 (0.009)	3.8 (0.024)	2.9 (0.018)
Denver	1.3 (0.008)	4.0 (0.025)	10.7 (0.068)	8.0 (0.051)

WIND PRESSURES DRIVING CAVITY AIRFLOW

Winds generate temporally and spatially varying pressures on building surfaces. These pressures are reported from field measurements, wind tunnel testing, and modeling, typically as nondimensional pressure coefficients. Straube (1998) used the differences in mean pressure coefficients measured on the surface of a small test building to estimate ventilation rates for a series of brick vent combinations. Inculet et al. (1997) measured pressure gradients, ΔP, on a building surface in a wind tunnel and divided the mean values by distance, L, and dynamic pressure, $0.5\rho U^2$(where ρ is the air density), to calculate gradient coefficients, as follows:

$$G = \Delta P / 0.5 L \rho U^2 \quad (2)$$

Predictions of surface pressure gradients using MCWS and Inculet's normalization approach are plotted in Figure 3 for a range of wind speeds. These results show a dramatic rise within 2.4 m (8 ft) of the wall edges. The edge of a tall building is predicted to have a 3.8 Pa/m (0.024 psf/ft) gradient in Edmonton and a 47.7 Pa/m (0.304 psf/ft) gradient in New York City. Midspan gradients are 0.5 and 6 Pa/m (0.003 and 0.038 psf/ft) for these cities. Values are tabulated in Table 3.

Cope et al. (2012) measured surface pressures on a small test house exposed to wind in a full-scale wind tunnel. The horizontal and vertical gradient results for winds perpendicular to the wall surface are plotted in Figure 4 for windward and leeward wall exposures.

Horizontal gradients range from 0.16/m to 0.43/m (0.05/ft to 0.13/ft) and vertical gradients range from 0.06/m to 0.27/m

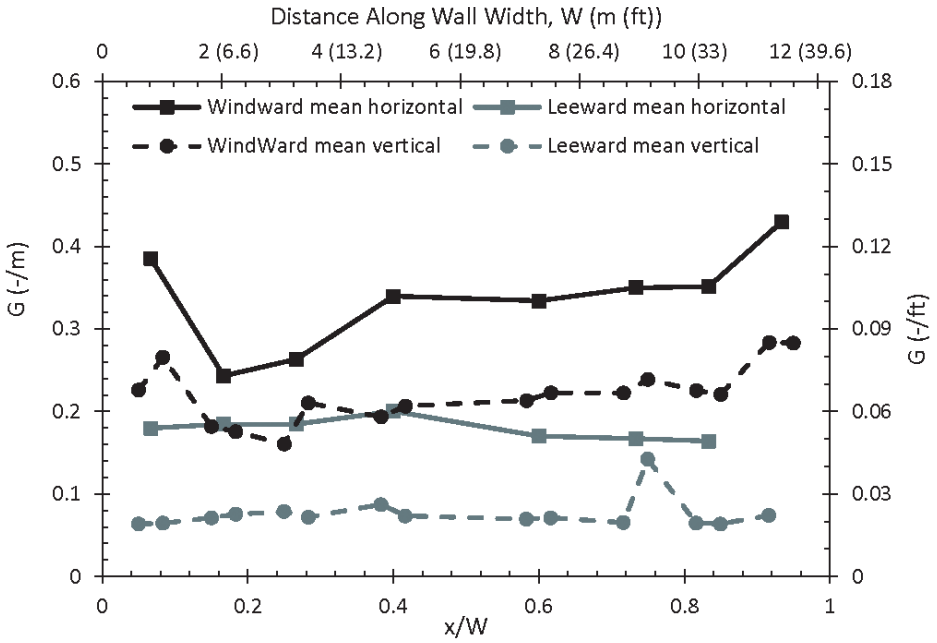

Figure 4 *Mean surface pressure gradients along width of wall for perpendicular wind.*

(0.02/ft to 0.08/ft). Using these results as "low" and "high" values, surface pressure gradients are plotted for a range of wind speeds in Figure 5 and tabulated in Table 4. Horizontal gradient values for a suburban house in Edmonton and a house in the countryside in New York City show as < 1 and 3–9 Pa/m (<0.006 and 0.019–0.057 psf/ft), respectively.

Cavity Pressure Gradients

Uvsløkk (1996) measured cavity pressure gradients of 0.1–0.5 Pa/m (0.001–0.003 pcf/ft) for mean wind speeds of 3 m/s (6.7 mph) in a 23 mm (~1 in.) clear air gap behind wood siding of a small test house. To determine cavity pressure coefficients for vinyl siding, the cavity pressure data, which were also available in Cope et al.'s (2012) data set, were analyzed. Horizontal and vertical cavity pressure gradients from this data set are shown in Figure 6. Average windward mean horizontal and vertical gradients across the width are 0.2/m and 0.1/m (0.06/ft and 0.03/ft). Both averages are significantly lower than the surface gradients.

CAVITY AIRFLOWS

Cavity pressure gradients can be used to calculate airspeeds using the Darcy-Weisbach equation and assuming the cavity flow is equivalent to fully developed laminar flow between parallel plates as follows:

$$\Delta P_c = \frac{96}{\mathrm{Re}} \cdot \gamma \frac{\rho V_c^2}{2} \cdot \frac{L}{D_h} \qquad (3)$$

where

ΔP_c = cavity pressure gradient

V_c = mean cavity velocity

γ = cavity blockage factor

Re = Reynolds number based on hydraulic diameter

D_h = hydraulic diameter

H = cavity depth

L = cavity length

Equivalent vertical and horizontal vinyl siding cavity depths of 1 and 4 mm (1/32 and 5/32 in.) from Van Straaten (2004) were used to estimate cavity velocities for a range of wind speeds, as shown in Figure 7. Wind speeds between 1.4 and 5.9 m/s (3 and 13 mph) correlate to horizontal cavity air speeds of 0.03 and 0.5 m/s (0.1 and 1.6 ft/s) and vertical air speeds of 0.004 and 0.06 m/s (0.01 and 0.2 ft/s).

Vinyl siding cavity flow rates based on measured cavity pressure coefficients are tabulated for five cold cities in Table 5. The vertical air speeds are quite low, whereas the horizontal air speeds are as high as 0.3 m/s (1 ft/s).

Field-measured hourly average cavity air velocity values for various cladding systems as high as 0.6 m/s (2 ft/s) have been published in previous studies, as shown in Table 6. The reported values are similar to those calculated for vinyl siding.

A complex model would be needed to estimate vinyl siding airflow rates given its complex vent opening geometry. Straube (1998) used simple pipe flow models to estimate cavity airflow rates for cladding systems with discrete vents in series with a cavity as follows:

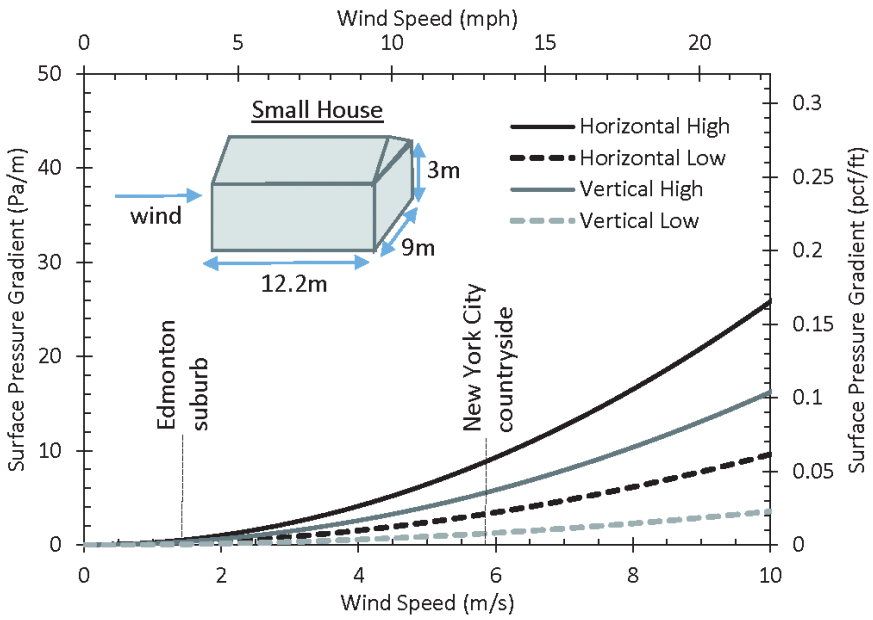

Figure 5 *Surface pressure gradients for range of measured small-house values.*

Table 4. Calculated Small-House Surface Pressure Gradients, Pa/m (psf/ft)

Location	Small House in Countryside				Small House in Suburbs			
	Low		High		Low		High	
	Horizontal	Vertical	Horizontal	Vertical	Horizontal	Vertical	Horizontal	Vertical
Toronto	1.4 (0.009)	0.5 (0.003)	3.8 (0.024)	2.4 (0.015)	1.0 (0.006)	0.4 (0.002)	2.7 (0.017)	1.7 (0.011)
Chicago	1.5 (0.009)	0.6 (0.004)	3.9 (0.025)	2.5 (0.016)	1.0 (0.007)	0.4 (0.002)	2.8 (0.018)	1.7 (0.011)
New York City	3.3 (0.021)	1.3 (0.008)	9.0 (0.057)	5.7 (0.036)	2.4 (0.015)	0.9 (0.006)	6.3 (0.040)	4.0 (0.025)
Edmonton	0.3 (0.002)	0.1 (0.001)	0.7 (0.005)	0.5 (0.003)	0.2 (0.001)	0.1 (0.0005)	0.5 (0.003)	0.3 (0.002)
Denver	0.7 (0.005)	0.3 (0.002)	2.0 (0.013)	1.3 (0.008)	0.5 (0.003)	0.2 (0.001)	1.4 (0.009)	0.9 (0.006)

$$\Delta P = C_{en} \cdot \frac{\rho V_{en}^2}{2} + \frac{96}{\mathrm{Re}} \cdot \gamma \frac{\rho V_c^2}{2} \cdot \frac{L}{D_h} + C_{ex} \cdot \frac{\rho V_{ex}^2}{2} \quad (4)$$

Entrance and exit loss coefficients, C_{en} and C_{ex}, were taken from duct design manuals and measured data. A number of assumptions have been made in the cavity flow calculations. Negligible inertial and compression effects are assumed. The use of absolute pressure gradients ignores air mixing within the cavity and assumes that all airflow completely clears the cavity. Davidovic et al. (2012) published a review of Straube's (1998) model observing that transition losses would exist between the vents and the cavity and would therefore resist the airflow. Using these simplifications should result in conservative (high) cavity velocities in this study. The model was found by Basset and McNeil (2009) to correlate well with cladding ventilation over the course of a day but not for shorter increments.

Analyses using this simple model have been replicated both for brick with limited ventilation consisting of a 25 mm (1 in.) cavity with 50% cavity blockage connecting 10 by 60 mm (3/8 by 2 1/2 in.) top and bottom vents and with good ventilation consisting of a 25 mm (1 in.) clear cavity with similar bottom vents and open top slot. A smooth panel over a 50 mm (2 in.) cavity with 12 mm (1/2 in.) slot opening has also been analyzed. The results are shown in Figure 8. It is noted that the model for the smooth panel is dominated by the pressure drop at the slot openings and hence is relatively independent of cavity height.

The minimally ventilated brick cavity (common in North America) is predicted to have low air speeds in most exposures. The cavity air velocity for the other claddings is tabulated for the same five cold cities in Table 7. The well-

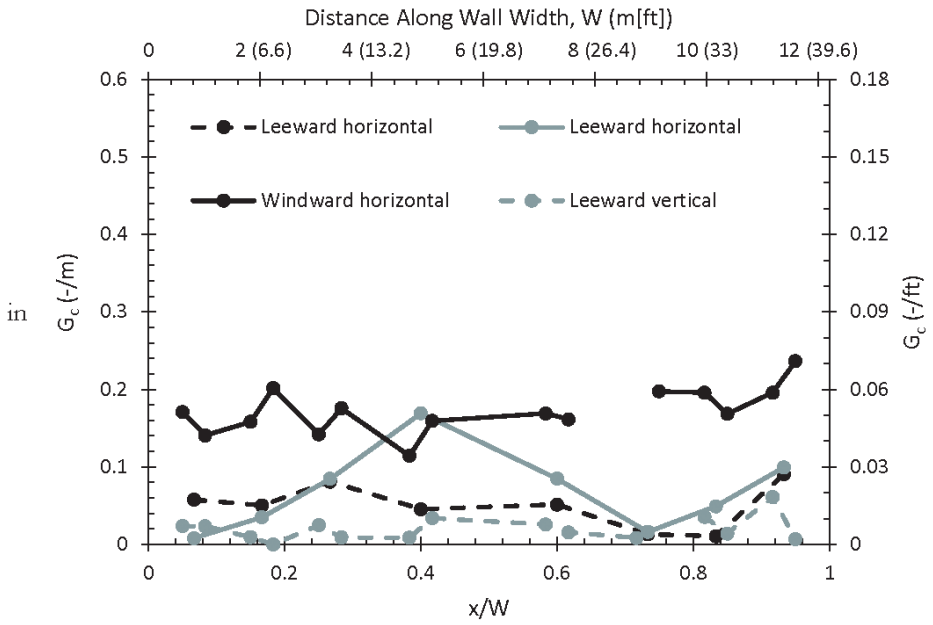

Figure 6 *Mean vinyl siding cavity pressure gradients along width of wall for perpendicular wind.*

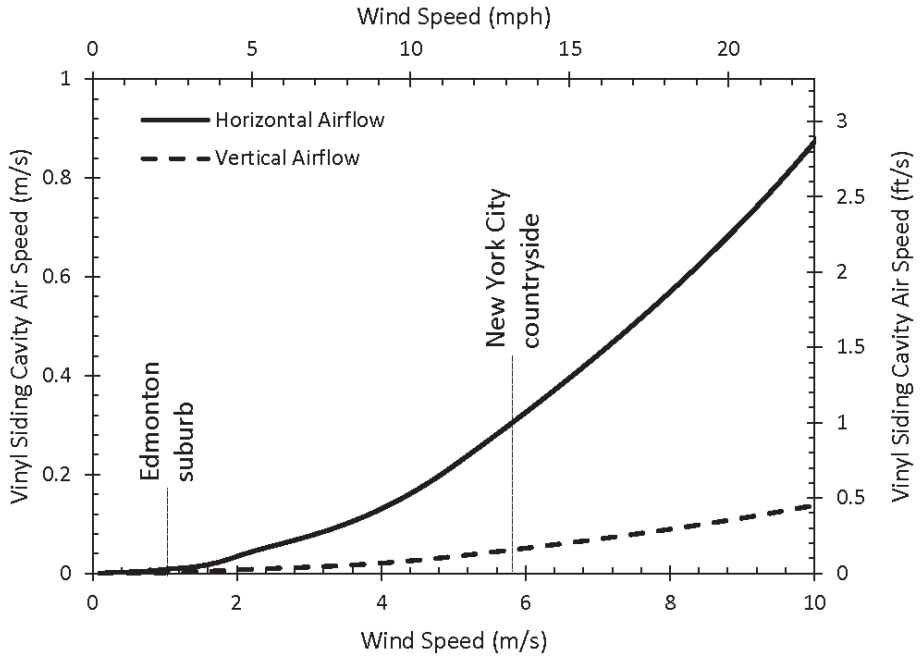

Figure 7 *Vinyl siding cavity airflow predicted from measurement of cavity pressure gradients.*

ventilated brick cases range up to 0.11 m/s (0.36 ft/s) cavity speed. The smooth panel cases with horizontal or vertical slots range up to 0.74 m/s (2.4 ft/s). In summary, the flow behind many types of cladding, when used on tall and exposed buildings or on a small suburban house, will fall with the lower end in the range of 0.1 to 1.0 m/s (0.33 to 3.3 ft/s). This range of cavity air velocities was used for the results presented in the next section.

EXPERIMENTALLY MEASURED WIND WASHING HEAT LOSS

Yarbrough and Tooe (1983) constructed a test rig to measure the impact of airflows over 152 mm (6 in.) of loose fill insulation. The tests included mineral wool with densities between 25 and 34 kg/m^3 (1.6 and 2.2 pcf). The results showed an increase in wind-washing-induced heat loss with decreas-

Table 5. Predicted Cavity Air Speeds for Vinyl Siding, m/s (ft/s)

Location	Small House in Countryside		Small House in Suburbs	
	Horizontal	Vertical	Horizontal	Vertical
Toronto	0.13 (0.43)	0.02 (0.07)	0.09 (0.30)	0.01 (0.03)
Chicago	0.13 (0.43)	0.02 (0.07)	0.09 (0.30)	0.02 (0.07)
New York City	0.30 (0.98)	0.05 (0.16)	0.21 (0.69)	0.03 (0.10)
Edmonton	0.02 (0.07)	0.004 (0.01)	0.02 (0.07)	0.003 (0.01)
Denver	0.07 (0.23)	0.01 (0.03)	0.05 (0.16)	0.01 (0.03)

Table 6. Measured Cavity Velocities Found in Literature, m/s (ft/s)

Reference	Cladding and Exposure	Mean Wind Speed	Mean Cavity Velocity
Schwartz (1973)	Open slots to 40 mm (1.5 in.) cavity behind smooth panels in 18-story building	0–8 m/s (0–26 ft/s)	0.2–0.6 m/s (0.7–2 ft/s)
Künzel and Mayer (1983)	Open slots to 20 mm (3/4 in.) cavity behind smooth panels in three-story building	3 m/s (10 ft/s)	0.06–0.16 m/s (0.2–0.5 ft/s)
Gudum (2003)	Top and bottom slot to 25 mm (1 in.) clear cavity in small single-story test building	0.7–2.1 m/s (2–7 ft/s)	0.12–0.27 m/s (0.4–0.9 ft/s)
Falk and Sandin (2013)	Open slots to 25 mm (1 in.) cavity behind smooth panels in single-story test building	2 m/s (7 ft/s)	0.05m/s (0.2 ft/s)

ing density. Extrapolating the results for densities of mineral wool insulation boards of 70 kg/m^3 (4.4 pcf) and greater would suggest negligible wind washing impacts at cavity airflows of 1 m/s (3 ft/s).

An apparatus was developed to measure the impact of cavity airflow on heat flow for a number of mineral wool insulation products as shown in Figure 9. The test approach and apparatus was similar to that of Yarbrough and Tooe (1983) but included several improvements, as follows:

- The meter section was surrounded with guard heaters maintained within ±0.02°C (±0.05°F) of the plate temperature to limit flanking losses.
- A thicker 6.4 mm (1/4 in.) aluminum plate was used for the meter section to encourage more even temperature distribution.
- A custom electric heating system using Omega-N160 nickel chromium heating wire was installed at to the bottom of the meter section's aluminum plate with fine spacing to further ensure temperature uniformity.
- A long 1625 mm (64 in.) guard length was installed upstream of the meter area to allow airflow disturbances and uneven air velocities at the air cavity entrance to dissipate before reaching the meter section (see Figure 9).
- For simplicity, a thick layer of insulation was used in lieu of a lower guard heater to limit heat loss in this direction.

To calculate the thermal conductance, U, of the test sample, the Fourier heat transfer equation is used:

$$U = [A \cdot (T_m - T_s)] / q \quad (5)$$

where

A = sample area
T_m = temperature of the meter plate below the sample
T_s = temperature of the top surface of the sample
q = heat flux

Multiple surface temperatures and the electrical heating system voltage and current were recorded at 5 min intervals with a Campbell Scientific CR1000 data acquisition system. The meter plate and the four side guard plates were constantly maintained at 60°C±0.02°C (140°F±0.05°F) during testing using a relay that was controlled by the CR1000. The heat flux through the sample was calculated as the electrical power provided to the meter plate minus flanking losses. The flanking losses were through the passive lower guard and were determined by a calibration procedure. Airflow velocity was measured by setting a Dwyer 641RM-12-LED air velocity transmitter with an accuracy of ±0.15 m/s (±0.5 ft/s) in the middle air cavity depth over the center of the meter plate. To factor out the effects of sample thermal resistance temperature dependence, a correction factor was applied to the airflow R-values based on Lasercomp FOX 314 heat flow

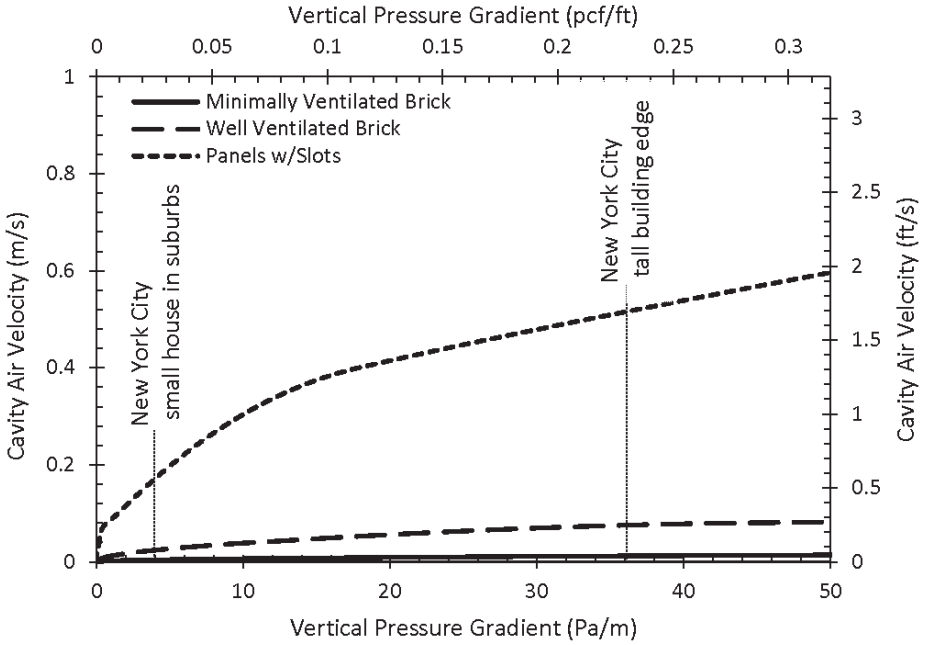

Figure 8 *Cavity air velocities for simple cladding systems.*

Table 7. Calculated Air Velocities behind Cladding, m/s (ft/s)

Location	Tall Building in City Centre			Small House in Countryside		Small House in Suburbs	
	Midspan	1–2 m	1 m Edge	Low	High	Low	High
Well-Ventilated Brick (Vertical Flow)							
Toronto	0.03 (0.10)	0.05 (0.17)	0.07 (0.24)	0.01 (0.04)	0.03 (0.09)	0.01 (0.04)	0.02 (0.08)
Chicago	0.03 (0.10)	0.05 (0.17)	0.07 (0.24)	0.01 (0.05)	0.03 (0.10)	0.01 (0.04)	0.02 (0.08)
New York City	0.05 (0.15)	0.08 (0.26)	0.11 (0.37)	0.02 (0.07)	0.04 (0.15)	0.02 (0.06)	0.04 (0.12)
Edmonton	0.01 (0.04)	0.02 (0.07)	0.03 (0.10)	0.01 (0.02)	0.01 (0.04)	0.005 (0.02)	0.01 (0.03)
Denver	0.02 (0.07)	0.04 (0.12)	0.05 (0.17)	0.01 (0.03)	0.02 (0.07)	0.01 (0.03)	0.02 (0.06)
Horizontal Slots—1 m (3.3 ft) Vent Separation							
Toronto	0.16 (0.52)	0.28 (0.92)	0.47 (1.54)	0.12 (0.39)	0.20 (0.65)	0.10 (0.32)	0.16 (0.54)
Chicago	0.16 (053)	0.29 (0.94)	0.48 (1.57)	0.12 (0.39)	0.20 (0.66)	0.10 (0.33)	0.17 (0.55)
New York City	0.25 (0.82)	0.44 (1.45)	0.74 (2.42)	0.18 (0.61)	0.31 (1.01)	0.15 (0.50)	0.26 (0.84)
Edmonton	0.07 (0.22)	0.12 (0.39)	0.20 (0.65)	0.05 (0.16)	0.08 (0.27)	0.04 (0.14)	0.07 (0.23)
Denver	0.11 (0.37)	0.20 (0.66)	0.34 (1.11)	0.08 (0.28)	0.14 (0.46)	0.07 (0.23)	0.12 (0.39)
Vertical Slots—1 m (3.3 ft) Vent Separation							
Toronto	0.16 (0.52)	0.28 (0.92)	0.40 (1.33)	0.07 (0.23)	0.15 (0.51)	0.06 (0.19)	0.13 (0.42)
Chicago	0.16 (0.53)	0.29 (0.94)	0.41 (1.36)	0.07 (0.24)	0.16 (0.52)	0.06 (0.20)	0.13 (0.43)
New York City	0.25 (0.82)	0.44 (1.45)	0.64 (2.08)	0.11 (0.36)	0.24 (0.80)	0.09 (0.30)	0.20 (0.66)
Edmonton	0.07 (0.22)	0.12 (0.39)	0.17 (0.56)	0.03 (0.10)	0.07 (0.21)	0.02 (0.08)	0.05 (0.18)
Denver	0.11 (0.37)	0.20 (0.66)	0.29 (0.95)	0.05 (0.17)	0.11 (0.36)	0.04 (0.14)	0.09 (0.30)

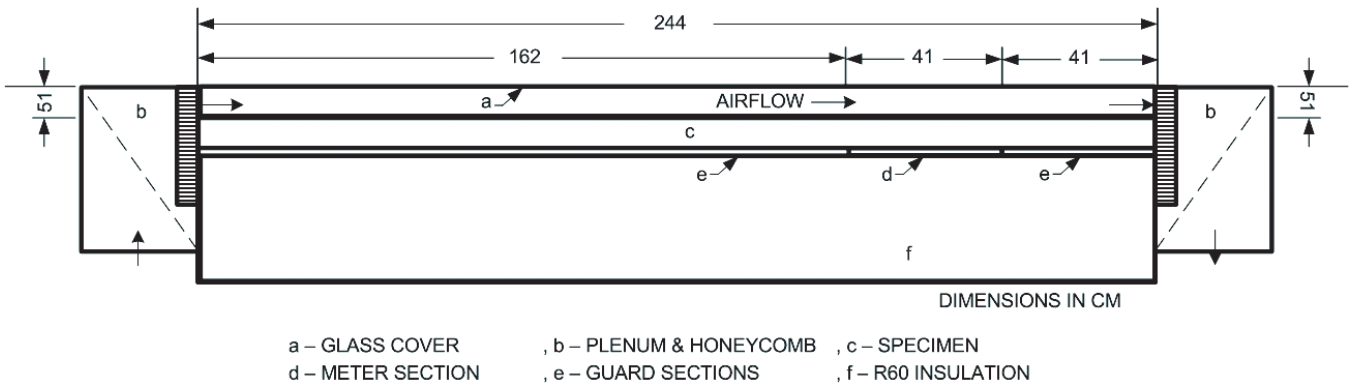

Figure 9 *Diagram of test apparatus.*

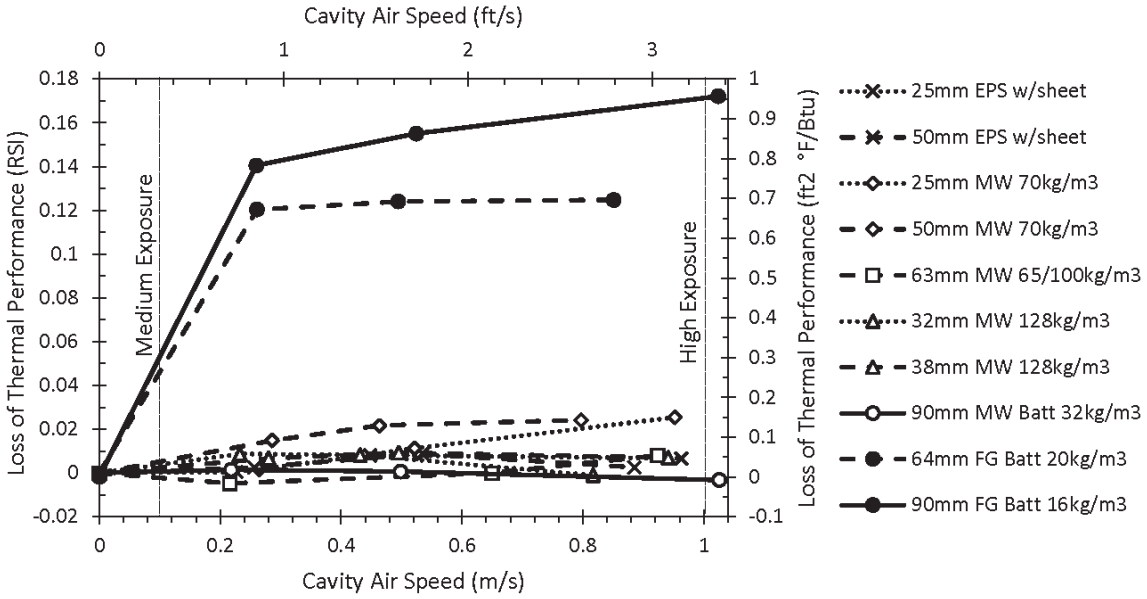

Figure 10 *Cavity air speed impact on absolute mineral wool board thermal performance.*

meter measurements. For a temperature difference of 20°C (68°F), the heat flow uncertainty was calculated to be ±0.02 W/m^2·°C (±10.0035 Btu/h·ft^2·°F). For insulations with RSI values from 0.65 to 2.47 (R-3.7 to R-14), this uncertainty is 0.02 to 0.08 RSI (R-0.1 to R-0.5).

The test results are plotted in Figure 10, showing measured loss of thermal performance for a range of cavity air speeds. The results for the various insulation materials tested are further tabulated in SI units in Table 8 and in I-P units in Table 9. The tables include rated, ASTM C518 (ASTM 2015) sample test results, test results from the wind washing test rig but with no applied airflow (still air), and estimated loss of thermal performance based on test results for 0.1 and 1 m/s (0.3 and 3 ft/s) cavity airflow. These air cavity speeds were selected as approximate medium and high wind exposures.

Plastic-film-faced expanded polystyrene (EPS) boards were used to verify the measurement process. These samples should not be affected by cavity airflow, as they have an air-impermeable facer and were installed with carefully taped joints. The maximum performance variation over the test range of air speeds was less than 0.01 RSI (R-0.05), and still air values were within 0.01 RSI (R-0.05) of ASTM C518 measurements.

Two fibreglass batt samples (low density and high air permeability) were used as products with known susceptibility to wind washing to confirm the ability of the apparatus to measure wind washing effects. The R-8 and R-13 rated fiberglass samples showed 0.12 and 0.17 RSI (R-0.7 and R-1) losses of thermal resistance, respectively, for 0.1 and 1 m/s (0.3 and 3 ft/s) cavity air speeds.

The 70 kg/m^3 (4.4 pcf) samples were the only mineral wool insulation boards tested showing measurable wind washing impact. The maximum 0.03 RSI (R-0.2) impact is within the range of estimated test uncertainty, which is assumed to

Table 8. Summary of Wind Washing Testing Results (SI)

Material	Product Description	Thickness	RSI (20°C) Rated	RSI (40°C) ASTM C518	RSI (45°C) Still Air	Loss of RSI	
						0.1 m/s	1 m/s
Plastic-faced foamboard	Type 1 EPS	25 mm	0.65	0.61	0.60	<0.01	<0.01
Plastic-faced foamboard	Type 1 EPS	50 mm	1.30	1.12	1.13	<0.01	<0.01
Mineral wool board	70 kg/m^3	25 mm	0.74	0.70	0.72	<0.01	0.03
Mineral wool board	70 kg/m^3	50 mm	1.11	1.35	1.41	0.01	0.03
Mineral wool board	128 kg/m^3	32 mm	1.89	1.64	1.65	<0.01	<0.01
Mineral wool board	128 kg/m^3	38 mm	0.90	0.92	0.93	<0.01	<0.01
Mineral wool board	65/100 kg/m^3	64 mm	1.08	1.04	1.06	<0.01	<0.01
Mineral wool batt	32 kg/m^3	90 mm	2.47	2.27	2.17	<0.01	<0.01
Fibreglass batt	R-8 rated	64 mm	1.41	1.12	1.29	0.12	0.13
Fibreglass batt	R-13 rated	90 mm	2.29	1.92	1.91	0.12	0.17

Table 9. Summary of Wind Washing Testing Results (I-P)

Material	Product Description	Thickness	R- (68°F)	R- (104°F)	R- (113°F)	Loss of R-Value	
			Rated	ASTM C518	Still Air	0.3 ft/s	3 ft/s
Plastic-faced foamboard	Type 1 EPS	1 in.	R-3.7	R-3.5	R-3.4	<0.05	<0.05
Plastic-faced foamboard	Type 1 EPS	2 in.	R-7.4	R-6.4	R-6.4	<0.05	<0.05
Mineral wool board	4.4 pcf	1 in.	R-4.2	R-4.0	R-4.1	<0.05	R-0.2
Mineral wool board	4.4 pcf	2 in.	R-6.3	R-7.7	R-8.0	R-0.05	R-0.2
Mineral wool board	8 pcf	1 3/8 in.	R-10.7	R-9.3	R-9.4	<0.05	<0.05
Mineral wool board	8 pcf	1 1/2 in.	R-5.1	R-5.2	R-5.3	<0.05	<0.05
Mineral wool board	4/6.2 pcf	2 1/2 in.	R-6.1	R-5.9	R-6.0	<0.05	<0.05
Mineral wool batt	2 pcf	3 1/2 in.	R-14.0	R-12.9	R-12.3	<0.05	<0.05
Fibreglass batt	R-8 rated	2 1/2 in.	R-8.0	R-6.4	R-7.3	R-0.7	R-0.7
Fibreglass batt	R-13 rated	3 1/2 in.	R-13.0	R-10.9	R-10.8	R-0.7	R-1.0

explain why the impacts on the 50 mm (2 in.) sample appear greater than those for the thinner 25 mm (1 in.) sample.

The test method was designed to provide a simple repeatable cavity flow scenario of eddy-free flow parallel to the insulation surface. It was also found during the study that installation care significantly affected the testing results for all samples. This observation suggests a significant impact of airflow paths through and beneath poorly installed insulated board insulations. It is noted that samples were installed with more care and against a flatter, more consistent surface than would be typical of field applications. Differences in flexibility and roughness of insulated sheathings could affect the vulnerability of such products to installation deficiencies. The effects of gaps between and behind samples is recommend for future studies.

It is assumed that openings are relatively small and that eddies within the wind are not carried into the cavity and the momentum of the wind is not impacting the material directly. Hypothetically, for large openings (such as slots larger than 50 mm [2 in.]) these phenomena could have significant scouring effects on fibrous insulations, increasing heat loss. These cases should be explored through further analysis and field measurements.

Finally, components causing partial blockages within the cavity may accelerate, redirect, and/or create eddy structures within the cavity airflow. It is assumed that such affects are

limited to small, narrow areas, limiting heat loss and interior surface temperature impacts.

CONCLUSION

A methodology for predicting wind washing impacts has been presented in this paper. It is proposed to use average winter wind speeds or MCWS for wind washing analysis. The use of wind speed adjustments for sheltering and height-effect-based building code structural wind load calculation have also been proposed. Air speeds as high as 0.74 m/s (1.7 ft/s) were predicted using simple airflow network analysis for well-ventilated brick cladding and slot panels, respectively. Analysis of full-scale wind cavity tunnel pressure tap data for a small house was used to predict vinyl siding cavity air speeds as high as 0.3 m/s (0.7 ft/s).

Heat flow measurements were taken for a number of mineral wool board products. The 25 and 50 mm (1 and 2 in.) thick 70 kg/m^3 (4.4 pcf) mineral wool board samples tested showed wind washing impacts to reduce thermal performance as much as 0.03 RSI (R-0.2). These values are small and practically negligible for design considerations.

ACKNOWLEDGMENTS

We would like to thank ROXUL Inc. for supporting and providing valuable input to this research. We would also like to thank Anne Cope and Murray Morrison from the Institute for Business and Home Safety for providing time series data from their full-scale wind tunnel tests.

NOMENCLATURE

α	=	exponent based on surface roughness
γ	=	blockage factor for the cavity
ρ	=	density of air
A	=	sample area
C	=	loss coefficients for the entrance and exit
D	=	hydraulic diameter of the cavity
DB	=	dry-bulb temperature
G	=	pressure gradient coefficient
h	=	height
L	=	cavity length
MCDB	=	mean coincident dry-bulb temperature (with 0.04% and 0.1% wind speed)
MCWS	=	mean coincident wind speed (with 99.6% design dry-bulb temperature)
ΔP	=	pressure difference
q	=	heat flux through sample
T	=	temperature
U	=	adjusted wind speed or thermal conductance of sample
V	=	air cavity air speed
W	=	wall width
WS	=	wind speed
x	=	horizontal distance from edge of wall

Subscripts

c	=	cavity
en	=	entrance
ex	=	exit
h	=	hydraulic
H	=	horizontal
m	=	meter
S	=	surface
V	=	vertical

REFERENCES

ASHRAE. 2013. *ASHRAE Handbook—Fundamentals*. Atlanta: ASHRAE.

ASTM. 2015. ASTM C518-15, *Standard test method for steady-state thermal transmission properties by means of the heat flow meter apparatus*. West Conshohocken, PA: ASTM International.

Bankvall, C. 1978. Forced convection: Practical thermal conductivity in an insulated structure under the influence of workmanship and wind. In *Thermal transmission measurements of insulations* (ASTM STP660), pp. 409–25. West Conshohocken, PA: ASTM International.

Bassett, M., and S. McNeil. 2009. Ventilation measured in the wall cavities of high moisture risk buildings. *Journal of Building Physics* 32(4):291–303.

Berlad, A., Tutu, R., Jaung, and Y. Yeh. 1979. *Interim progress report on an investigation of energy transport in porous insulator systems, ORNL/SUB-7551/I.* Oak Ridge, TN: Oak Ridge National Laboratory.

Cope, A., J. Crandell, D. Johnston, V. Kochkin, Z. Liu, L. Stevig, and T. Reinhold. 2012. Wind loads on components of multi-layer wall systems with air-permeable exterior cladding. *Proceedings of the ATC-SEI Advances in Hurricane Engineering Conference.*

Davidovic, D., J. Piñon, E. Burnett, and J. Srebric. 2012. Analytical procedures for estimating airflow rates in ventilated, screened wall systems (VSWS). *Building and Environment* 47:126–37.

Deseyve, C., and T. Bednar. 2005. Increased thermal losses caused by ventilation through compact pitched roof constructions—In situ measurements. *Proceedings of the 7th Symposium on Building Physics in the Nordic Countries* 2:881–87.

Falk, J., and K. Sandin. 2013. Ventilated rainscreen cladding: Measurements of cavity air velocities, estimation of air exchange rates and evaluation of driving forces. *Building and Environment* 59:164–76.

Gudum, C. 2003. Moisture transport and convection in building envelopes—Ventilation in light weight outer walls. Doctoral thesis, Technical University of Denmark, Lyngby, Denmark.

Henning, G.N. 1983. Energy conservation with air infiltration barriers. In *Thermal insulation, materials, and systems for energy conservation in the '80s* (ASTM

STP789), pp. 551–58. West Conshohocken, PA: ASTM International.

Hens, H., A. Janssens, and W. Depraetere. 2001. Hygrothermal performance of masonry cavity walls with very low U-factor: A test house evaluation. *Proceedings of Thermal Performance of the Exterior Envelopes of Whole Buildings VIII International Conference.*

Inculet, D., D. Surry, and A. Davenport. 1997. Unsteady pressure gradients and their implications for pressure equalized rainscreens. *ICBEST'97 Conference Proceedings.*

Janssens, A., and H. Hens. 2007. Effects of wind on the transmission heat loss in duo-pitched insulated roofs: A field study. *Energy and Buildings* 39(9):1047–54.

Künzel, H., and E. Mayer. 1983. Untersuchung über die notwendige Hinterlüftung an Außenwandbekeidung aus großformatigen Bauteilen. Schriftenreihe Bundesminister für Raumordnung, Bauwesen, und Städtebau; 3.

Schwarz, B. 1973. Witterungsbeansphruchung von Hochhausfassaden, HLH Bd. 24, 12:376–84.

Silberstein, A., E. Auguis, and D. McCaa. 1991. Forced convection effects in fibrous thermal insulation. In *Insulation materials: Testing and applications*, vol. 2 (ASTM STP1116), pp. 292–309. West Conshohocken, PA: ASTM International.

Straube, J. 1998. Moisture control and enclosure wall systems. Doctoral thesis, University of Waterloo, Waterloo, Ontario, Canada.

Straube, J. 2001. Air flow control in building enclosures; More than just air barriers. *Proceeding of 8th Buildingg Science & Technology Conference*, pp. 282–302.

Tanner, C., and K. Ghazi. 1996. Warmebrucken von hinterlufteten Fassaden. EMPA Bericht 158 740, Dubendorf.

Taylor, B., and A. Philips. 1983. Thermal transmittance and conductance of roof construction incorporating fibrous insulation. In *Thermal insulation, materials, and systems for energy conservation in the '80s* (ASTM STP789), pp. 479–501. West Conshohocken, PA: ASTM International.

Uvsløkk, S. 1996. The importance of wind barriers for insulated timber frame constructions. *Journal of Building Physicss* 20(1):40–62.

Van Straaten, R. 2004. Ventilation of cladding systems. Master's thesis, University of Waterloo, Waterloo, Ontario, Canada.

Yarbrough, D., and L. Tooe. 1983. Effects of air movement on thermal resistance of loose-fill insulation. In *Thermal insulation, materials, and systems for energy conservation in the '80s* (ASTM STP789), pp. 529–41. West Conshohocken, PA: ASTM International.